

Photothermal measurements of absorption in LBO with a “proxy pump” calibration technique

A. Alexandrovski*^a, A.S. Markosyan^b, H. Cai^c, M.M. Fejer^b

^aStanford Photo-Thermal Solutions, Pahoa, HI, USA 96778-8240, ^bE.L. Ginzton Laboratory, Stanford University, Stanford, CA, USA 94305-4088, ^cGamdan Optics Inc., 2362 Qume Drive, San Jose, CA, 95131-1844

ABSTRACT

Photothermal technology provides sensitive detection of the optical absorption in bulk materials and coatings. To obtain the absolute absorption numbers it requires a proper calibration. In this work a new, “proxy pump” calibration approach is described. The proxy pump has a wavelength at which the material exhibits high enough optical absorption to be evaluated via direct loss measurements. The pump beam is shaped to have the same spot size as the main pump at which the optical absorption of the material is to be determined. Once the thermal field in the material has the same profile both with the proxy and main pump, the sample is self-referenced. Consecutive tests with proxy and main pumps provide absolute absorption numbers. LBO crystals are notorious objects for which the photothermal response is not easy to calibrate since the material has very low absorption in the UV, visible and near IR. In order to calibrate these materials using the above approach we used 2.3 μm laser as a proxy pump. At this wavelength LBO absorbs more than 15 % per cm length. For crystals oriented in XY and YZ planes the photothermal response was found to be 3 times weaker than for Schott glass NG12 with the same amount of absorbed power. With this correction, NG12 glass that has absorption more than 45 %/cm in the wide range of wavelengths can be used as a reference calibration material for LBO crystals.

Keywords: Photothermal technology, calibration, LBO crystal.

1. INTRODUCTION

Photothermal absorption measurements which utilize an optical probe is a proven way to test various optical components with high sensitivity¹. The indirect nature of these measurements when the thermal effect on the probe comes via index of refraction change and/or surface bending requires some proper calibration of the signal. In this contribution we focus on the bulk absorption calibration technique for the widely used nonlinear optical material LBO².

1.1 Experimental setup

A standard Photothermal Common-path Interferometer³ (PCI) instrument had been used for the measurements. The 2310 nm single TE00 mode Fabry-Perot 40 mW laser diode from Brolis Semiconductors was added to the setup as a “proxy pump”. The polarization of this pump was set vertical, same as the polarization of probe, in order to minimize walk-off effects for the birefringent samples. The focal spot size estimated by the knife-edge technique was 65 μm . The M^2 parameter value was 1.5. The combination of the M^2 value and the relatively long wavelength resulted in the Rayleigh range being as short as 1.5 mm. That proved to be a limiting factor for the measurements as discussed later.

It is worth mentioning that the 2310 nm wavelength should work with many other materials which have substantial absorption at this wavelength: BBO, CLBO, Calcite, BK7 glass, etc. Direct evaluation of the absorption loss for all uncoated crystals and for the reference sample, 3.58 mm-thick Schott glass NG12, had been made with the same PCI setup. The Thorlabs thermal sensor S401C with the claimed linearity $\pm 0.5\%$ had been used for transmission measurements. The experimentally verified repeatability for these measurements was better than $\pm 2\%$. In order to subtract Fresnel reflections refractive indices for all samples have been derived from available literature data. Although the data at 2310 nm are missing the reasonable estimates can be made based on the index dispersion of the materials used. Fortunately, even the 0.01 error in the estimate of the index contributes less than 1% relative error to the calculated absorption value. The following refractive index values were used: $n_z = 1.577$ and $n_x = 1.542$ for LBO, $n_o = 1.634$ for BBO and $n = 1.479$ for the NG12 glass.

1.2 Calibration approaches

A variety of calibration methods were used throughout the history of photothermal absorption measurements. In the case of PCI technology these are:

- all-theoretical;
- all-experimental;
- universal reference with correction factors;
- proxy pump (the current contribution is the first report on the technique).

The all-theoretical approach relies on the exact solutions for the oscillating thermal field generated by the chopped pump and calculation of the diffraction effects that shape the distorted probe wavefront. The corresponding solutions exist in the form of Bessel functions for the thermal field⁴ and Fresnel integral or Gaussian beam propagation for the optical part of the task³. The problem with this approach is the availability and accuracy of the properties of a material that factor into the response.

The easiest case for calculations is when the bulk absorption response is dominated by the temperature dependence of the refractive index, the one for the zero stress (mechanically free), zero electric field situation, $\beta^{E,\sigma}$. This property is commonly known as the $\partial n / dT$. One example of the “calculable” material is the fused silica glass. The contribution to the index change from local strains in the heated area is small because fused silica has relatively weak thermal expansion. All the material properties required for calculations, thermal conductivity, thermal diffusivity, refractive index dependence on temperature, and, sure enough, the refractive index itself, are known with sufficient precision. As a rule of a thumb the thermal expansion effects could be neglected when the coefficients of thermal expansion (CTE) are several times smaller than the $\partial n / dT$.

LBO with its large and anisotropic thermal expansion exemplifies the opposite situation. Also the material is a pyroelectric. Therefore the electric field and stresses cannot be neglected in LBO. The full expression for the index of refraction change with temperature is

$$\Delta n(\Delta T, E, \sigma) = \beta^{E,\sigma} \Delta T - \frac{n^3}{2} r^\sigma E - \frac{n^3}{2} \pi^E \sigma \quad (1)$$

when the thermodynamic parameters are temperature T , electric field E , and stress σ , or

$$\Delta n(\Delta T, E, \sigma) = \beta^{E,S} \Delta T - \frac{n^3}{2} r^S E - \frac{n^3}{2} p^E S \quad (2)$$

when the strain S is chosen instead of stress. Here $\beta^{E,S}$ is the index of refraction change for the zero field, mechanically clamped (zero strain) material, r^σ and r^S are the linear electrooptic coefficients for the mechanically free and mechanically clamped situations, π^E and p^E are the piezooptic and elasto-optic constants. To calculate stresses and the electric field, mechanical and electrostatic equations have to be used with stiffness tensor components, CTE, piezoelectric and pyroelectric constants. Most of these are known with poor precision or even not reported in the literature. This makes all-theoretical calculations impossible for LBO.

The all-experimental concept implies relative measurements of absorption when tests of a given sample and a reference are made for the same pump. The reference should be made of the same material, with the same orientation in case of anisotropic crystal, but with known absorption. An example of this approach in the past was the usage of lightly doped Ti-sapphire at 1064 nm⁵. There are at least two problems with this way of calibration: first, the reference sample should have big enough absorption which means it is a somewhat modified material, doped, reduced, etc. Second, to find and keep references for every material at every wavelength of test is a hard endeavor.

LBO has very low absorption in the UV, visible and near IR. Attempts to find a sample with big absorption did not bring any result in 15 years.

So far the most widely exploited calibration technique for the PCI technology was the universal reference. The universal reference material should have a reasonably big absorption, preferably in the range of 0.2 to 2 cm⁻¹, covering broad spectrum. The transmission spectrum of the Schott glass NG12 has been measured with the Cary 500 spectrophotometer and converted into absorption spectrum using the refractive index data from Schott⁶.

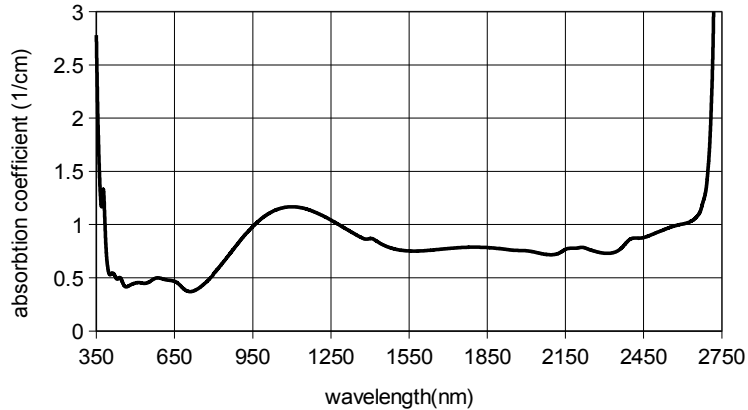


Figure 1. Absorption spectrum of Schott glass NG12.

Within the range 350 nm to 2650 nm the absorption of the glass falls into the comfortable margin. However, to use it when testing different materials correction factors (CF) should be applied. The CF accounts for differing material properties, in the case of anisotropic materials it also depends on orientation. The experimental evaluation of the CF could be done at any wavelength, one time. Still, this procedure requires the sample of the tested material with absorption known at that single wavelength. The CF is not wavelength dependent but depends, albeit weakly, on the parameters of the setup. The analysis of this dependence for LBO is given in the subsequent part of this contribution.

In order to apply the universal reference with CF approach to LBO one has to look for the wavelength at which LBO absorbs naturally. Based on the sketchy data provided by some LBO manufacturers the range of interest is between 2 and 3 microns. Since the corresponding pump laser is to be used only for calibration we use the term “proxy pump” for it. The proxy pump beam has to be shaped to have the same focal spot size as the main pump at which the optical absorption of the material has to be determined. Once the thermal field in the material has the same profile both with the proxy and main pump, the sample is self-referenced. Consecutive tests with proxy and main pumps provide absolute absorption numbers. Combined with the universal reference plus CF method the proxy pump has to be used only once to establish the value of the CF.

2. EXPERIMENTAL DATA

2.1 NG12 glass

The direct measurement of absorption loss in the glass at 2310 nm was done with the same 3.58 mm-thick sample that had been used over years as the universal reference. The derived value of absorption coefficient, 0.682 cm⁻¹, the repeatability being 4%, corresponds fairly to the spectrophotometer data, Fig.1.

The longitudinal photothermal scan through the glass shows the effect of pump depletion, Fig.2. The front surface of the sample corresponds to 2 mm distance on the recorded trace. The bumps surrounding both surfaces are diffraction effects, the artifact of the PCI technology.

In Fig.3 the corrected graph is plotted. The value of the “responsivity” is derived from the central part of the trace unaffected by the surface effects. The responsivity of the setup to a certain object tested for the bulk absorption is defined as the modulation depth of probe per unit of power absorbed over 1 cm length. The responsivity is an integral characteristic of the setup but depends also on the properties of the tested material.

The estimated relative error for the responsivity given all the instruments involved in the measurements was 9%.

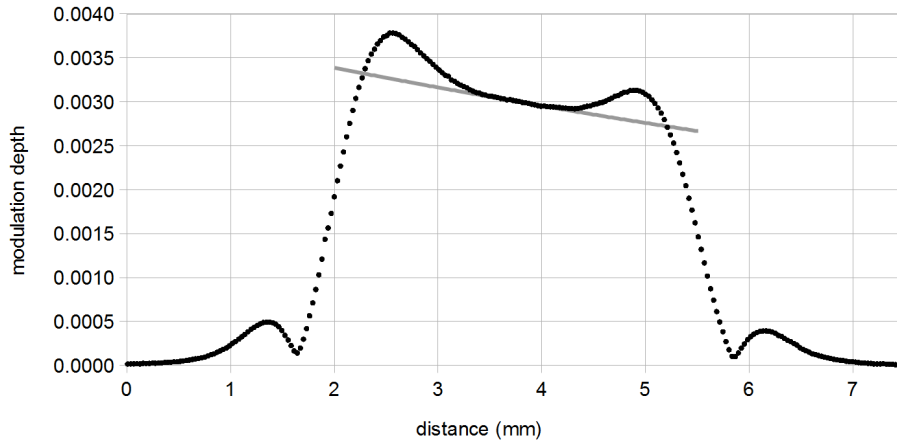


Figure 2. NG12 glass, longitudinal scan. Black dots: modulation depth of probe. Gray line: calculated effect of pump depletion.

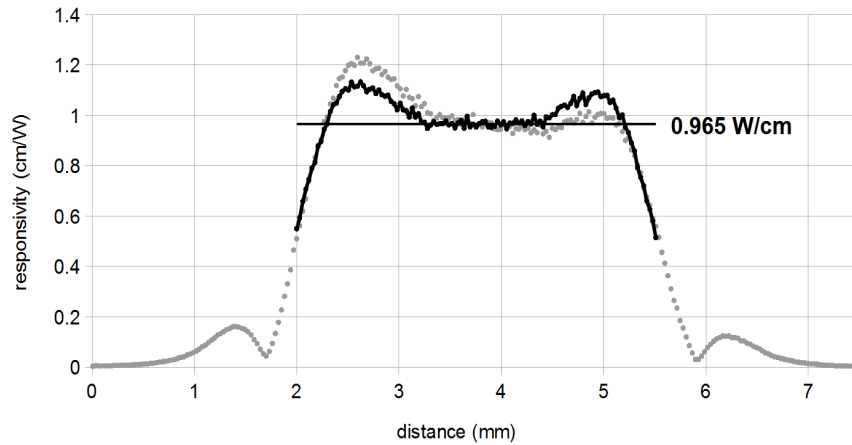


Figure 3. NG12 glass. Gray dots: responsivity as-is. Black dots: responsivity corrected for the pump depletion. Horizontal line: the averaged responsivity value.

2.2 LBO, XY-plane cut

Although we did not find good data on the nature of absorption in the vicinity of 2310 nm in LBO the FTIR data point to the fundamental, multi-phonon absorption at this wavelength rather than to any defect-associated absorption⁷. The proxy pump and red HeNe probe polarization were set parallel, normal to the pump/probe crossing plane. An X-cut, 10 mm-long, uncoated LBO sample mounted with the Z-axis along the polarization direction was used to quantify the absorption at 2310 nm. The value 0.335 cm^{-1} had repeatability better than 3%.

The repeated longitudinal scans made on different dates, Fig.4, show good stability of the photothermal signal. Another thing to note is the somewhat steeper slope of the bulk absorption signal as compared to the calculated effect of pump depletion.

The adjustment of the data to the pump depletion effect, Fig.5, did not completely remove the slope on the bulk absorption data. This effect had been attributed to the gradual shift of the focal plane of the pump relative to probe, see discussion in the corresponding section. The value of responsivity had been deduced by averaging data points from 2.5 to 4 mm segment of data on the adjusted plot. Given the scatter of data and all instrumental errors the total error for the responsivity value 0.228 W/cm is 7.5% relative. When compared with the NG12 glass value this number results in the CF of 3.1 ± 0.4 .

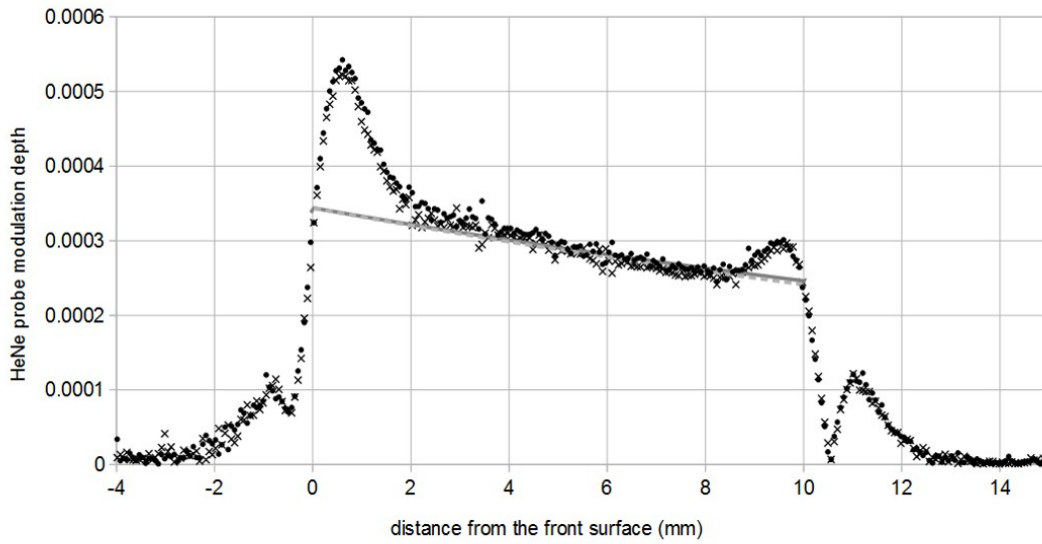


Figure 4. Probe modulation depth for the X-cut, uncoated LBO sample. Black circles and crosses: two scans at different dates. Gray line: the effect of pump depletion. Gray dashed line: the depletion effect with absorption 2%, relatively, larger than for the solid gray line.

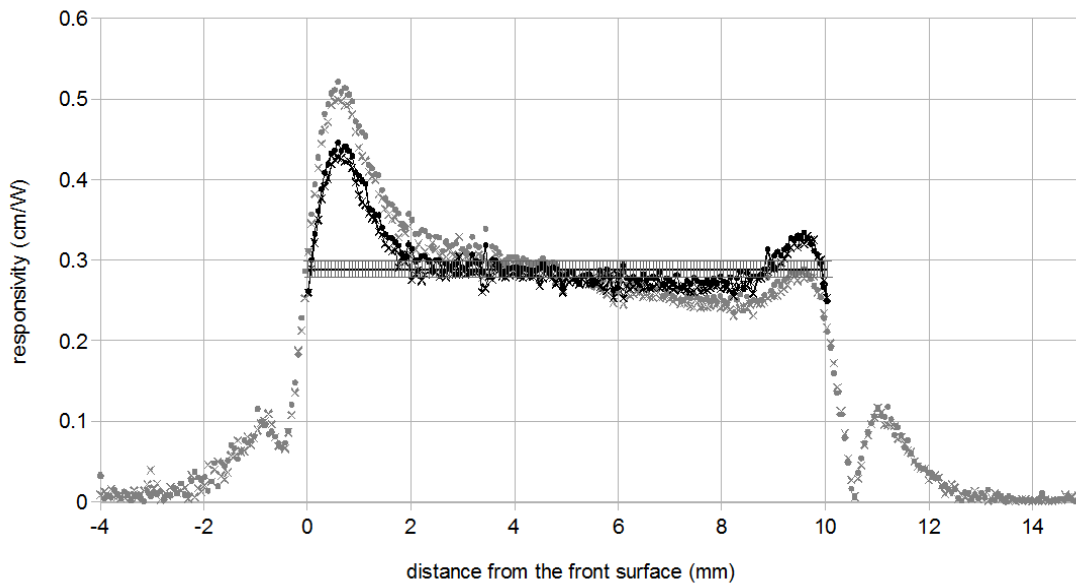


Figure 5. Responsivity plot for the X-cut, uncoated LBO sample, replotted data from Fig.4. Gray dots and crosses: responsivity as-is. Black dots: responsivity corrected for the pump depletion. Horizontal line: the averaged responsivity value showing the error bars.

The longer, 30 mm-long, LBO sample, a 32.5° cut in the XY-plane, had correspondingly stronger effect of the focal plane shift, Fig.6. Again, the value of responsivity had been deduced by averaging data points from 2.5 to 4 mm segment of data taken from the adjusted plot. The derived responsivity 0.268 W/cm had an accumulated error of 8%. The CF value 3.0 ± 0.4 applies to this sample.

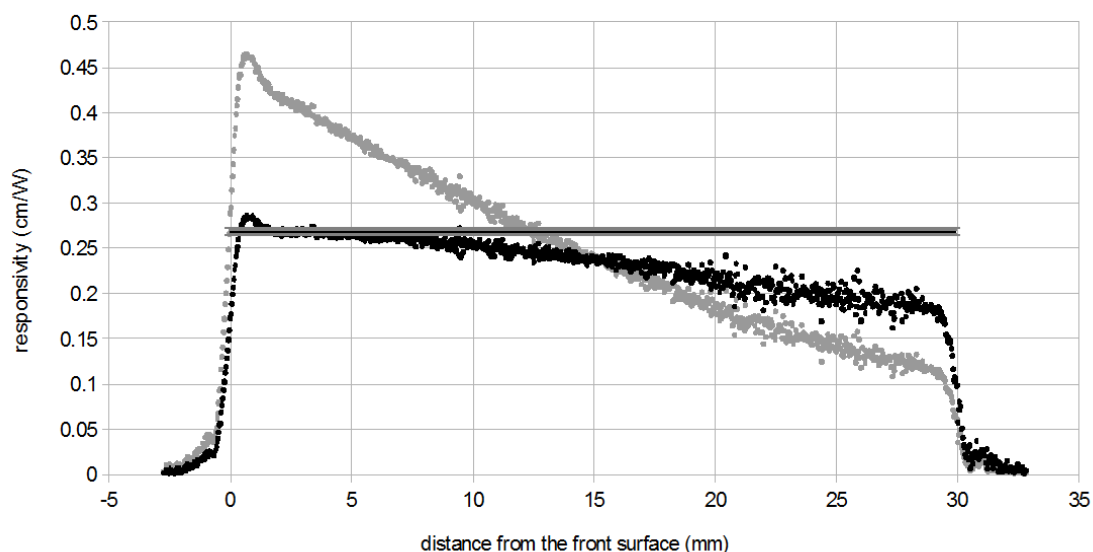


Figure 6. Responsivity plot for the 30 mm-long, AR-coated LBO cut at 32.5° in the XY-plane . Gray dots: responsivity as-is. Black dots: responsivity corrected for the pump depletion. Horizontal line: the averaged responsivity value with error bars.

2.3 LBO, YZ-plane cut

For this orientation samples had been placed with X-axis of LBO parallel to the polarization direction with YZ-plane of crystal being in the plane of pump/probe crossing. An uncoated sample, 10 mm-long, cut at 43.7° to the Z-axis had been used to determine the absorption coefficient. The value 0.183 cm^{-1} had repeatability better than 4%.

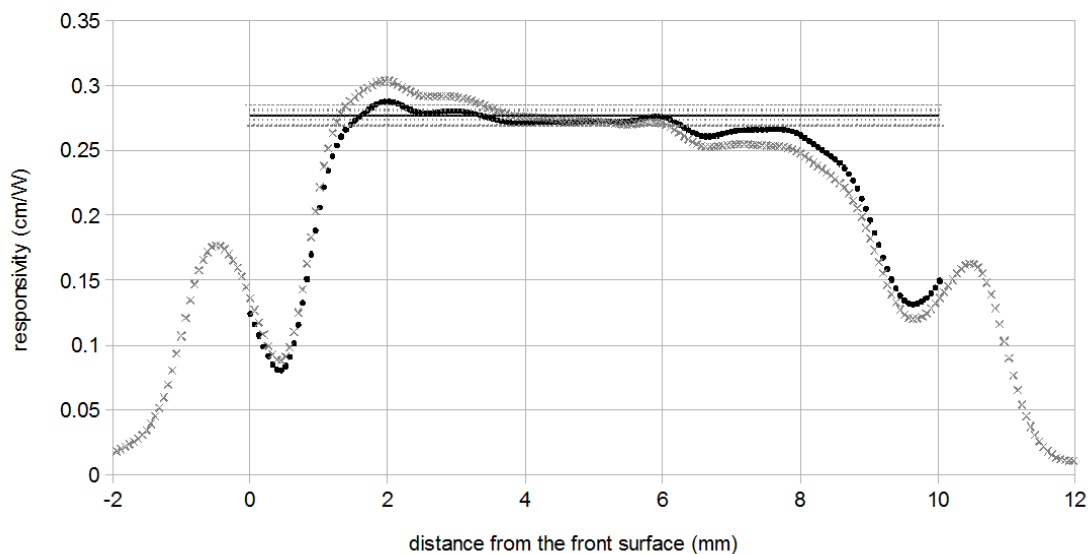


Figure 7. Responsivity plot for the 10 mm-long, uncoated LBO, cut at 43.7° to the Z-axis. Gray dots: responsivity as-is. Black dots: responsivity corrected for the pump depletion. Horizontal line: the averaged responsivity value with error bars.

The averaged responsivity taken again by averaging data points from 2.5 to 4 mm segment of data amounted to 0.276 W/cm , the calculated CF was 3.2 ± 0.5 . The unusual shape of the photothermal signal near surfaces, with the dips instead of bumps is discussed later.

2.4 BBO

A single, uncoated BBO crystal had been tested same way as LBO samples. The orientation of the 10 mm-long sample was 50.3° to the optical axis of the crystal. The sample was placed with the optical axis perpendicular to the pump/probe crossing plane, parallel to polarization of pump and probe.

The value 0.714 cm^{-1} for the absorption coefficient was found from the direct loss measurements.

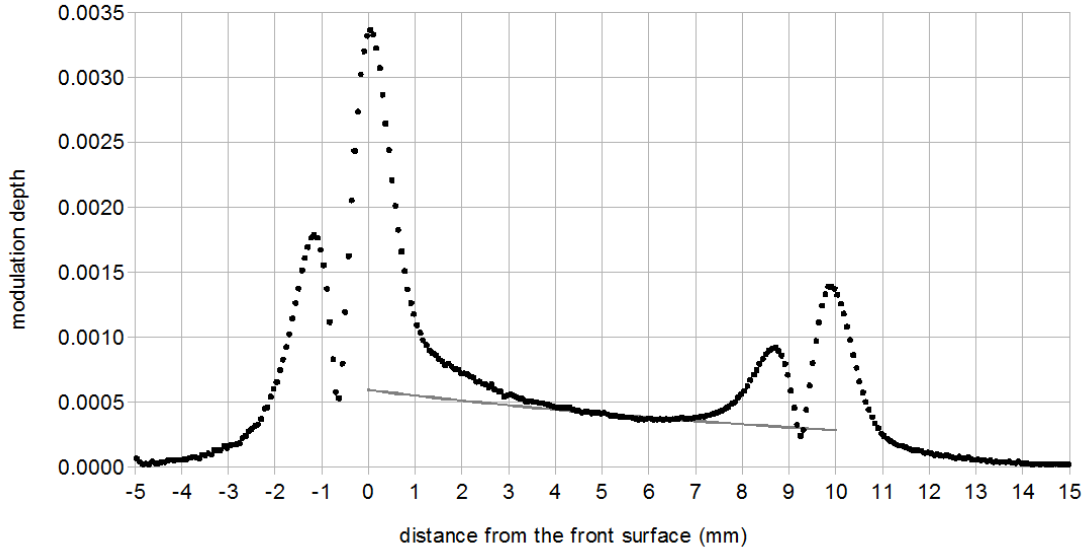


Figure 8. Probe modulation depth plot for the 10 mm-long, uncoated BBO cut at 50.3° to the optical axis. Black dots: modulation depth. Gray line: the calculated pump depletion effect.

Strong anomalies of the photothermal signal near surfaces leave little space to estimate the responsivity. Note that these anomalies are generated by the bulk absorption, not by the increased absorption of the surface layers. Tentatively, the CF was estimated to be 4.1.

2.5 1064 nm tests

The uncoated LBO crystals were tested for absorption at 1064 nm with a 9 W CW laser. In Fig.9 absorption signal spikes correspond to surfaces. Unlike 2310 nm scans, the surface anomalies do correspond to excessive absorption in thin surface layers. The bulk absorption signal is visible between spikes. The wavy behavior of the bulk absorption is due to unfiltered noise equivalent to about 1 ppm/cm of absorption for this scan. The averaged absorption coefficient value between spikes is 5.6 ppm/cm for the Z-axis polarized pump and 4.7 ppm/cm for the polarization of the pump in the XY-plane. The error of these measurements was dominated by the random noise of the signal, ± 0.8 ppm/cm.

Absorption spikes at surfaces develop for uncoated LBO crystals as a result of prolonged exposure to humid air. The surface spikes have to be calibrated separately. We did not establish the calibration for LBO surfaces yet. So far we have to apply the generic calibration which means the standard PCI reference, fused silica substrate coated with semi-transparent Inconel layer, is the source of calibration. To apply it to spikes on the 1064 nm scans the maximum value for the spike should be divided by the factor of, approximately, 60. The corresponding surface absorption values are well below 1 ppm then for the Fig.9.

YZ-cut LBO, Fig.10, had been scanned through with different polarization of the pump at different locations. Because for the degrading surfaces absorption varies a lot across the aperture surface absorption spikes are not the same. The averaged absorption between spikes is 5.8 ppm/cm for the X-axis polarized pump and 6.6 ppm/cm for the polarization of the pump in the YZ-plane.

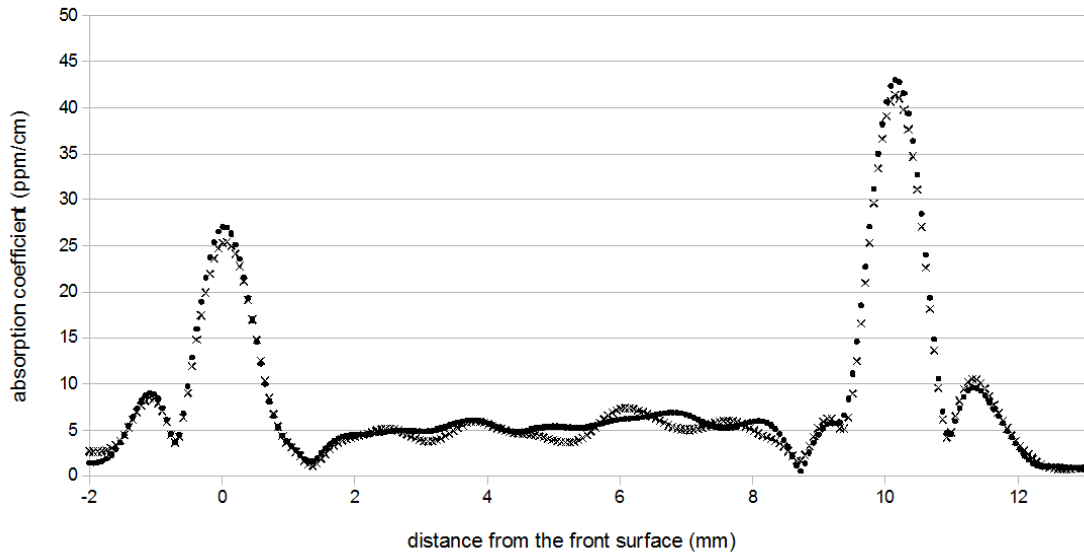


Figure 9. Consecutive longitudinal scans at 1064 nm for the X-cut, uncoated LBO sample. Scans recorded for the same path. Dots: pump polarization along Z-axis. Crosses: pump polarization in the XY-plane of the crystal.

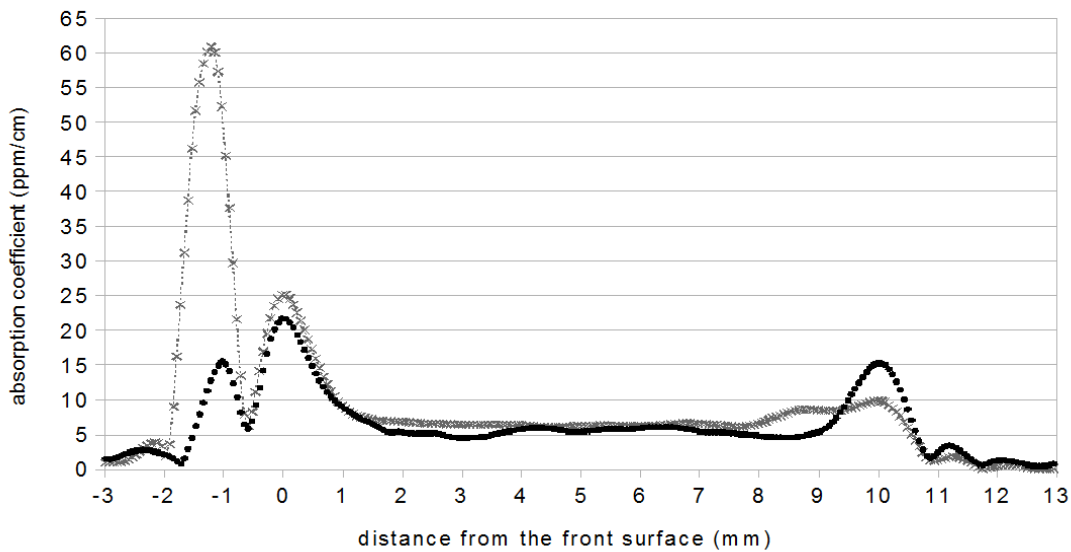


Figure 10. Longitudinal scans at 1064 nm for the YZ-plane-cut, uncoated LBO sample. Scans recorded for different paths. Dots: pump polarization along X-axis. Crosses: pump polarization in the YZ-plane.

3. DISCUSSION

3.1 Correction factor

The proxy pump approach requires some scrutiny if used only once to establish the correction factor (CF) for a given material/orientation. Several parameters of the PCI system could vary between instruments and users. The question is how steady is the value of the CF when these parameters change. The answer is given in the Table 1. All dependencies are theoretical estimates other than the frequency response one. The largest change of the CF happens when the

modulation frequency of the pump is altered. However, the change is reasonably small while the parameter itself is an easily controlled one.

Table 1. The dependence of responsivity and CF for LBO crystal to small changes of the PCI setup parameters.

Parameter of the setup	Value	Deviation from the value	Responsivity change	Correction factor change
Pump spot size	75 μm	10%	-3.1%	0.6%
Probe spot size	230 μm	10%	3.1%	-0.6%
Chopper frequency	390 Hz	5%	-9.6%	1.0%
Observation distance	10 mm	10%	0.5%	-1.6%
Photodetector aperture	1 mm	10%	-4.5%	-0.1%

The results for the direct absorption tests and photothermal measurements at 2310 nm are summarized in the Table 2. When repeated measurements of absorption had been made the corresponding error margin is shown. The error for the CF is an accumulated error from all instruments used for measurements plus repeatability error.

The last column in the table shows the sign of the thermal lens as detected by the PCI setup. Although literature data point to negative values of the $\partial n_z / dT$ property⁸ the positive thermal lensing effect had been detected when the polarization of probe coincided with the Z-axis of LBO. That can only be explained by dominating contribution of strains, via elasto-optic effect, to the effective value of the index change.

Table 2. Absorption and correction factors for the tested crystals.

Sample description	Orientation	Length, mm	Probe polarization	Absorption at 2.3 μm , 1/cm	Correction factor with NG12 glass as a reference	Sign of thermal lens
LBO X-cut, uncoated	$\Theta = 90^\circ$; $\varphi = 0^\circ$	10.46	z	0.335 +/- 0.07	3.1 +/- 0.4	+
LBO Type I, AR-coated	$\Theta = 90^\circ$; $\varphi = 32.5^\circ$	30.48	z	0.334	3.0 +/- 0.4	+
LBO Type II, uncoated	$\Theta = 43.7^\circ$; $\varphi = 90^\circ$	10.34	x	0.183 +/- 0.06	3.2 +/- 0.5	-
LBO Type II, AR-coated	$\Theta = 51.8^\circ$; $\varphi = 90^\circ$	20.40	x	0.187	3.1 +/- 0.5	-
BBO, uncoated	$\Theta = 50.3^\circ$	9.985	o	0.741	4.1	-

3.2 Effects leading to index of refraction change

The nature of the refractive index change caused by local heating is worth analyzing together with the reaction of the optical probe to this change.

As expressions (1,2) show the electric field and stresses/strains within and around the heated area contribute to the overall index change. The expression (2) is more suitable for the analysis. It has to be complimented with the expressions for strain and the polarization density change

$$S = \alpha^E \Delta T + d E + s^E \sigma, \quad (3)$$

$$\Delta P = \gamma^\sigma \Delta T + \varepsilon_0 (\varepsilon^\sigma - 1) E + d \sigma \quad (4)$$

where α^E are the coefficients of thermal expansion measured at zero electric field, d represents the piezoelectric tensor, s^E is the elastic compliance tensor, γ^σ is the pyroelectric coefficient at zero stress, ϵ^σ is the dielectric permittivity.

The thermal expansion and the pyroelectric effect generate strains and spontaneous polarization change in the crystal. The resulting electric field and local stresses could be found solving corresponding coupled electrostatic and elastostatic problems. Fortunately, many significant conclusions may be derived without these calculations from the symmetry of the situation.

If to neglect the divergence of the pump beam the heated area isotherms will have the shape of an elliptic cylinder with the longitudinal axis defined by the direction of the beam. The ellipticity arises from the anisotropy of the thermal conductivity. Both XY and YZ planes of LBO are the planes of symmetry which defines the orientation of the ellipse and places constraints on other effects that depend on the properties of the material.

It can be shown then that in the plane containing the axes of intersecting pump and probe the electric field of the pyroelectric origin will be exactly in that plane where the pump propagates, XY or YZ, depending on the orientation of LBO. In other words, the plane of symmetry does not allow for the component of the field orthogonal to the corresponding plane to exist.

Next, the electric field direction in the plane where pump propagates, XY or YZ, should be orthogonal to the direction of the pump beam. Any polarization created along the direction of the pump beam, for example the component $\Delta P_1 = d_{16}\sigma_6$, see Eq.4, in case of XY plane, will not produce a significant electric field in the bulk. The corresponding field will appear at or near surfaces where the beam enters and exits the crystal. Another way to see it is to consider the translational symmetry for the limit of the infinitely long crystal. Every plane orthogonal to the pump beam direction should be equivalent in terms of any parameter including the electric potential, hence no field in the direction of the pump.

Next, the integral over the probe path for the electric field component parallel to the probe beam direction is zero when the probe comes from, and ends up, at the same electric potential, away from the heated area. That is true when probe crosses pump deep in the bulk, see Fig.11, but not true when they cross near any surface.

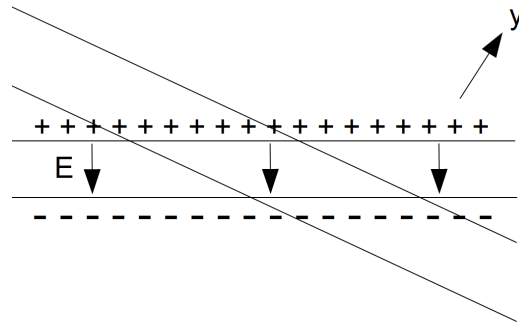


Figure 11. Schematic representation of the electric field orientation in XY or YZ plane of the LBO crystal with the pump shown as propagating horizontally and the probe coming at an angle to the pump in the corresponding plane. Arrow labeled Y shows the direction of the polar axis of the crystal.

Moreover, the component of the electric field orthogonal to the direction of the probe beam is integrated to zero as well just because its value is proportional to the collinear component at any location. As a result all terms of the electrooptic contribution to the index change in expression (2) $-\frac{n^3}{2}r^S E$ do not contribute to the photothermal signal when pump and probe cross deep in the bulk in the XY or YZ plane of the crystal.

The translational symmetry considerations nullify also the linear strain in the direction of the pump beam. The shear strain components containing this direction are canceled by the plane of symmetry, XY or YZ. Only linear strains in the plane orthogonal to the pump beam direction survive as well as the shear in this plane, s_6 for the XY plane and s_4 for

the YZ plane. Shear strains do not affect the indices of refraction of interest in LBO. The elasto-optic contribution, Eq.2, to the index n_z , for example, is $-\frac{n_z^3}{2}(p_{31}^E S_1 + p_{32}^E S_2 + p_{33}^E S_3)$.

The last simplifying circumstance is analogous to how the electric field is integrated by the probe: the integral over any component of linear strain in the pump/probe mid-plane is zero because deep in the bulk the probe comes from and, upon crossing the heated area, ends up in the location with the zero displacement field.

The overall result of all symmetry considerations is the effective index of refraction change

$$\Delta n_z = \beta_3^{E,S} \Delta T - \frac{n_z^3}{2} p_{33}^E S_3 \quad (5)$$

for the XY plane of LBO and

$$\Delta n_x = \beta_1^{E,S} \Delta T - \frac{n_1^3}{2} p_{11}^E S_1 \quad (5)$$

for the YZ plane.

The solution for the elastic strains in isotropic materials⁸ shows that the tangential component of strain generated by the thermal expansion of a small cylindrical area of the material will be the only one strain component to be integrated by probe to a non-zero value. The total effective tangential strain for this case is $S_t = \frac{(1+\nu)}{(1-\nu)} \alpha \Delta T$ where ν is the

Poisson ratio. The integral over the probe path is the product of this strain S_t and the diameter of the heated area as if the material is free to expand with the only correction coming from the Poisson ratio. One may expect that similar situation applies to the anisotropic material but with the orientation dependent Poisson ratio.

The expressions (5,6) have the index of refraction change vs temperature for mechanically clamped, short-circuited material as the first term and a single strain-related addition as the second one. That second term, namely, the value of the corresponding strain, looks to be the single source of the dependence of CF on the angle of the cut within a given plane of the crystal. The dependence may be quite strong because thermal expansion is very different for the Y-axis, even the sign of the effect is different from other axes. Our data, within the accuracy of measurements, do not show this dependence though suggesting that the impact of this term is relatively small.

3.3 Anomalies of the photothermal signal near surfaces

The anomalies visible on longitudinal scans, Fig.7,8, for example, are associated with the electric field and mechanical strain distributions near surfaces that are different from the bulk area. Another factor contributing to the difference is how the probe integrates the field and the strain. Even without the electric field component normal to a surface the probe will sense the presence of the electric field. Better knowledge of material parameters like the pyroelectric coefficient and electrooptic coefficients is needed to be able to model the response.

The strange shape of the signal near surfaces of the YZ-cut LBO could be explained by the surface anomaly having the opposite sign with respect for the bulk absorption signal. This anomaly is not associated with any excess absorption in the surface layer but with the different response of the probe to the same bulk absorption.

When the crystal is coated or surfaces have an excess absorption because of defects or contamination the surface spikes appear on longitudinal scans that look different from the anomalies generated by the bulk absorption, Fig.9,10. That points to the future task of calibrating surface signal for various orientations of LBO as being quite tough. The dependence on orientation could be much stronger and the electrical conductivity of the surface layer may alter the response.

3.4 Focal plane shift for the 2310 nm pump

The drop of the pump depletion-corrected photothermal signal with the depth inside the LBO crystal could be explained by the big difference of refractive indices for the pump and the probe. The indices of LBO at 633 nm, the wavelength of the probe, are $n_z = 1.616$ and $n_x = 1.574$. Their values at 2310 nm were estimated as $n_z = 1.577$ and $n_x = 1.542$. For every 10 mm of the sample length the accumulated shift of the focal plane of the pump relative to the pump/probe crossing point is about 0.4 mm. Rayleigh range for the 2310 nm pump being as short as 1.5 mm the signal will drop as the diameter of the pump increases at the pump/probe crossing. This effect will be much smaller at 1064 nm and shorter wavelength because of the longer Rayleigh range.

4. CONCLUSIONS

The proxy pump approach

- is a useful experimental way to establish absolute absorption scale;
- eliminates the need to increase absorption at the wavelength of test (to easily detectable level) by modifying the material, for example, by introducing defects;
- is a one-time procedure when combined with a universal reference (correction factor is established).

The correction factor for LBO, with Schott glass NG12 as the reference, is 3.1 +/- 0.5 for any orientation of the crystal in XY and YZ planes.

REFERENCES

- [1] Bialkowski, S. E., [Photothermal Spectroscopy Methods for Chemical analysis], John Wiley & Sons, New York, Chemical analysis series, 134 (1996).
- [2] Chen, C., Wu, Y., Jiang, A., Wu, B., You, G., Li, R., and Lin, S., "New nonlinear-optical crystal: LiB_3O_5 ," J. Opt. Soc. Am. B 6(4), 616-621 (1989).
- [3] Alexandrovski, A., Fejer, M., Markosyan, A., Route, R., "Photothermal common-path interferometry (PCI): new developments," Proc. SPIE 7193, 71930D (2009).
- [4] Jackson, W. B., Amer, N. M., Boccara, A. C., and Fournier, D., "Photothermal deflection spectroscopy and detection," Appl. Opt. 20(8), 1333-1344 (1981).
- [5] Alexandrovski, A., Fejer, M., Route, R., "Effect of annealing on the light absorption in sapphire," AIP Conf. Proc. 523, 395-397 (2000).
- [6] As of year 2017 the ND12 glass had been removed from the active list by Schott Corporation but is still available from some vendors. The Schott North America website <http://www.us.schott.com/d/advanced_optics> lists NG12 glass as "will be manufactured if there is sufficiently high demand". The properties of the glass including refractive indices were available for download in the past, when the glass was being produced, and is now available from the authors of this contribution.
- [7] Kovacs, L., Polgar, K., Agnes, P., Capeletti, R., "FT-IR spectroscopy of OH ions in borate single crystals," Mikrochim. Acta [Suppl] 14,523-524 (1997).
- [8] Tang, Y., Cui, Y., and Dumm, M.H., "Thermal dependence of the principal refractive indices of lithium triborate," J. Opt. Soc. Am B 12(4), 638-643 (1995).
- [9] Young, W. C., Budynas, R. G., [Roark's Formulas for Stress and Strain], McGraw Hill Professional, 763 (2001).